

Multi-Paradigm Modeling of Mode I&II Dynamic Fracture Mechanisms in Single Crystal Silicon

by

Alan Cohen

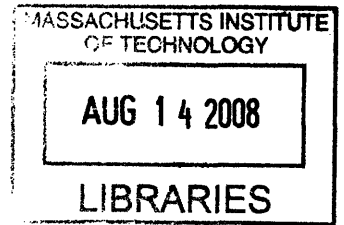
SUBMITTED TO THE DEPARTMENT OF MECHANICAL ENGINEERING IN
PARTIAL FULFILLMENT OF THE REQUIREMENTS FOR THE DEGREE OF

BACHELOR OF SCIENCE
AT THE
MASSACHUSETTS INSTITUTE OF TECHNOLOGY

JUNE 2008

©2008 Alan Cohen. All rights reserved.

The author hereby grants to MIT permission to reproduce
and to distribute publicly paper and electronic
copies of this thesis document in whole or in part
in any medium now known or hereafter created.



Signature of Author: _____
Department of Mechanical Engineering
May 9, 2008

Certified by: _____
Markus Buehler
Esther and Harold E. Edgerton Assistant Professor
Thesis Supervisor

Accepted by: _____
John H. Lienhard V
Professor of Mechanical Engineering
Chairman, Undergraduate Thesis Committee

Multi-Paradigm Modeling of Mode I&II Dynamic Fracture Mechanisms in Single Crystal Silicon

by

Alan Cohen

Submitted to the Department of Mechanical Engineering on May 9, 2008
in partial fulfillment of the requirements for the Degree of
Bachelor of Science in Mechanical Engineering

ABSTRACT

In addition to its semi-conducting properties, silicon has the ability to be manipulated with high precision at very small length-scales. This property makes it very useful in the design of Nano-/Micro-Electromechanical Systems (N/MEMS) and similar technologies. The understanding of fracture of silicon is crucial for the engineering process and the development of robust devices. However, the mechanisms of fracture in silicon are complex and are still not fully understood. Several experimental studies of fracture have been reported, however, these often lack insight into atomistic mechanisms of fracture. Ab initio computational methods (e.g. based on Density Functional Theory) to study silicon that are able to provide a fundamental description of the complex fracture mechanisms remain an open challenge. In particular, the mechanisms that lead to brittle cleavage or to the transition to ductile behavior of silicon at higher temperatures remains an open question. Empirical molecular dynamics (MD) studies have proven successful in simulating silicon fracture, but are unreliable and most models could not be validated against experimental results.

Here we propose to use MD modeling based on a novel first principles reactive force fields ReaxFF, which has shown to be an accurate model to describe fracture processes of silicon. Two numerical methods are used here to study fracture mechanisms in silicon: a multi-paradigm model employing reactive and non-reactive force fields, and a fully reactive model. The CMDF and GRASP are used for the simulation of brittle fracture mechanisms in mode I and mode II loading conditions, as well as simulations of the brittle-to-ductile transition (BDT). Our results indicate that CMDF is suitable for modeling silicon brittle fracture, but has limitations during the study of the mechanisms involved in the BDT. GRASP provides a suitable framework for BDT study, and the results in this study provide for the first time an observation of the BDT without the use of an empirical model. In this thesis we report, for the first time, the direct atomistic simulation of the BDT in silicon, revealing the microscopic atomistic mechanisms that explains this drastic change in the behavior of silicon.

Thesis Supervisor: Dr. Markus Buehler

Title: Esther and Harold E. Edgerton Assistant Professor

Table of Contents

Title Page	Page 1
Abstract	2
Table of Contents	3
Table of Figures	4
Chapter 1. Introduction	6
1.1 Silicon Fracture	6
1.2 Brittle-Ductile Transition in Silicon	7
1.3 Historical Modeling Attempts	7
Chapter 2. Literature Review	9
2.1 Modeling Brittle Fracture in Single Crystal Silicon	9
2.2 Modeling the Brittle-Ductile Transition	10
Chapter 3. Computational Methods	13
3.1 Computational Materials Data Facility (CMDf)	13
3.2 General Reactive Atomistic Simulation Program (GRASP)	14
3.3 Method to Observe Mode I&II Brittle Fracture	14
3.4 Method to Observe Brittle-Ductile Transition	16
Chapter 4. Results	18
4.1 Crack initiation for mode I loading	18
4.2 Crack initiation for mode II loading	21
4.3a Brittle Ductile Transition: CMDf Simulations	25
4.3b Brittle Ductile Transition: GRASP Simulations	26
Chapter 5. Discussion	33
5.1 Mode I & II Crack Growth During Brittle Fracture	33
5.1.1 Asymptotic Stress Fields Analysis	33
5.2 Brittle-Ductile Transition During Mode I Loading	38
Chapter 6. Conclusions	40
Bibliography	41

Table of Figures

Figure 1: Crack propagation with a pure Tersoff potential (a) and the hybrid ReaxFF-Tersoff model (b) along the [110] direction. The blue regions are Tersoff atoms, the red regions are reactive atoms. Subplot (c) shows the difference in large-strain behavior between Tersoff and ReaxFF. Both descriptions coincide at small strain. Reprinted with permission from [12].	10
Figure 2: The CMDF software uses a transition region for simulations that employ multiple inter-atomic potentials for the description of atomic bonds and interactions. Shown here is the model used for combining the ReaxFF and Tersoff potentials in the simulation of a silicon crystal. Reprinted with permission from [12].	14
Figure 3: Orientation of the crystal structure for the simulations, and the geometry of the initial crack, and reactive and non-reactive force fields.	15
Figure 4: This snapshot is taken from a mode I loading simulation during crack extension.	19
Figure 5: This snapshot is taken from a mode I loading simulation prior to crack extension. At 1.0689 ps (bottom left) it is possible to see the formation of 5 and 7-member rings. One pair is highlighted in red.	20
Figure 6: The steady-state crack velocity for the mode I loading case is approximately 3.3km/s. This result is taken from the time-averaged plot of the magnitude of the crack velocity.	21
Figure 7: This snapshot is taken from a mode II loading simulation prior to crack extension. The reactive region can be seen in yellow, and the non-reactive region is shown in blue. The initial deviation of the crack extension 45 degrees to the left can be observed in the bottom two snapshots.	22
Figure 8: This snapshot is taken from a mode II loading simulation during crack extension. The angle of crack growth direction is approximately 30-40 degrees.	23
Figure 9: A void begins to form initially ahead of the crack tip before steady-state crack growth occurs. The arrow points towards the void, and is also pointing in the direction where crack extension will occur.	24
Figure 10: The steady-state crack velocity for the mode II loading case is approximately 2.8 km/s (red dashed line).	25
Figure 11: These snapshots are taken from a mode I test at 900K. The formation of voids occurs ahead of the crack tip prior to crack extension.	26
Figure 12: The events during the simulation of a silicon crystal under tension at 1200K are indicative of brittle fracture. There is no indication of a brittle-ductile transition.	27

Figure 13: These snapshots are fracture events during a simulation at 1000K. The snapshots are carried out farther than was observed at 1200K. Void formation and coalescence can be seen at 5.570 ps and 6.700 ps. 29

Figure 14: These snapshots are fracture events during a simulation at 1500K. At 5.290 ps crack tip blunting begins to occur. 30

Figure 15: A simulation at 1500K, but slower strain rate, shows evidence of the BDT. . 31

Figure 16: Shown here is the Burgers circuit drawn around the dislocation that is emitted at 29.280 ps 32

Figure 17: This snapshot of the 300K simulation at a mode I strain rate of 0.00002% per fs, shows that brittle fracture occurs..... 32

Figure 18: This is the coordinate system used for the LEFM asymptotic stress field model. 34

Figure 19: Angular variations (σ) of the asymptotic stress field solutions for a stationary crack during mode I loading 36

Figure 20: Angular variations (σ) of the asymptotic stress field solutions for a static crack during mode II loading. 37

1. Introduction to Silicon

Silicon is the second most abundant element in the Earth's crust, after oxygen [1]. It plays an important role in many different applications: It can be found in nature as a structural element in certain organisms, and it plays a vital role in the growth of certain plant species [2, 3]. In the construction industry, it is a vital constituent of concrete, cement, glass, and stone. Its most interesting applications are the roles it takes in the manufacturing and the design of high-tech devices. In addition to its semi-conducting properties, silicon has the ability to be manipulated with high precision at very small scales. This property makes it very useful in the construction of N/MEMS devices and similar technologies [4].

1.1 Silicon Fracture

As length scales decrease, it becomes increasingly important to have accurate knowledge of material and mechanical properties. Continuum mechanics theory, used to describe the failure of materials, describes matter as being indivisible and continuous at the smallest length scale [5]. Material inhomogeneities are approximated, and theoretical predictions are confirmed by experiments. This method to describe the mechanical properties of materials, however, is limited because it does not give a fundamental perspective on the effects of phenomena that occur at an atomistic scale. These phenomena may include voids, dislocations, vacancies, and grain boundaries. These types of phenomena are on the order of 100nm and less, which makes continuum mechanics unfavorable when trying to describe the behavior of materials during failure, fracture, and deformation at that length scale [6].

In silicon semiconductor design, the smallest feature set can be on the order of 10nm, which makes it necessary to understand the properties and behavior of silicon at that level. The failure mechanics of semiconductors, and silicon in general, is extremely important as nano-scale devices are being developed that may interact directly with the human body. Crack formation and fracture at these length scales needs to be understood and predictable: creating a valid model for silicon fracture is vital before can be relied upon in critical or life-saving applications. In addition to the inability of continuum mechanics to properly describe atomistic-scale phenomena, there is an added difficulty in creating an accurate model of silicon due to its anisotropic crystal structure. Many traditional fracture mechanics models are based on

assumptions of isotropy, which adds another element of inaccuracy wherein silicon is involved. Research has already shown that continuum mechanics alone is insufficient in the analysis of the failure of single silicon crystals [7].

The simplest solution to this dilemma would be to abandon the convention that matter can indefinitely be sliced into smaller bits and create an atomistic model that treats matter as discrete units, or atoms. Atomistic modeling can provide insight into behavior at the nano-scale, which in turn would allow the formation of a more accurate theoretical model. Molecular dynamics simulations based on atomistic models can solve the equations of motion for a system of atoms or particles. The output for such a simulation results in a description of the position, velocity, and relative energies for all the particles in a system. This would be a critical development in the study of silicon fracture, and its understanding would lead to important advancements in the construction of nano-scale devices.

1.2 Brittle-Ductile Transition in Silicon

Experimental research has shown that under certain loading conditions and temperatures, silicon undergoes a drastic change in failure mode from brittle to ductile failure. This transition has implications in the construction and manufacture of nano-scale devices, and understanding it is vital to sustain the development of these types of technologies. Experimental research currently lacks the necessary precision to probe materials at the atomistic level, which would be necessary to begin the construction of a theoretical framework that can reliably predict the causes of a drastic phenomenon referred to as the brittle-ductile transition (BDT). Thus far, the mechanisms of BDT are not fully understood, particularly the changes in the material's behavior.

1.3 Historical Modeling Attempts

Developing a model to predict the mechanics and fracture behavior of silicon is not a novel concept. Molecular dynamics simulations have been used since the 1980s to predict the mechanical behavior of solids. Molecular dynamics (MD) methods model the atom as a point mass and use inter-atomic potentials, or force fields, to predict the interactions between atoms under different conditions. This method makes it particularly successful because it does not require any assumptions about the dynamics of material defects—materials behavior is

completely determined by interactions between individual atoms.

Most existing atomistic models of fracture depend upon the use of empirical parameters to describe the interaction between atomic bonds stretching and the associated forces [8]. These models are inaccurate in cases where there may be a breakdown of these empirical relationships: namely in experiments where significant stresses and strains may develop. In these cases it is necessary to use a quantum mechanical (QM) treatment of the bond behavior.

In MD, it is possible to use the ReaxFF reactive force field to correctly model behavior that requires QM treatments. Reactive inter-atomic potentials have the ability to describe the chemical interactions of bond behavior; in the context of materials fracture this is particularly important to be able to capture the phenomena associated with non-linear elasticity effects in brittle material fracture. The drawback with using reactive potentials is their computational inefficiency: in current computational environments, only several hundred or thousand atoms can be simulated at a time. Many phenomena associated with materials fracture can only be captured when observing the large-scale interactions of atoms, on the order of tens or hundreds of thousands of atoms.

The research presented here implements a novel approach that combines highly accurate, but computationally expensive reactive potentials, with less expensive non-reactive potentials in a hybrid computational facility. This approach allows multi-scale simulations to be developed whereas tens of thousands of atoms can be correctly modeled.

2. Literature Review

Brittle fracture in silicon has been a subject to many research efforts because of its complex nature and important applications. It is important to note several recent developments in the study of the dynamic behavior of silicon, specifically studies of brittle fracture and the BDT. In the next few paragraphs is a summary of important progress that has been made over the past decades.

2.1 Modeling Brittle Fracture in Single Crystal Silicon: A Grand Challenge

Sherman 2006 [7] depicts the complex nature of single crystal silicon fracture: crack propagation is associated with individual bonds at a plane of propagation. Continuum methods are shown to lack the ability to reproduce atomistic-scale phenomena. These phenomena include threshold crack speeds, minimum crack velocities, crack deflection from one cleavage plane to another, and the preferred cleavage planes during rapid fracture. Continuum mechanics idealizes materials as isotropic, continuum, and homogeneous. The author shows that this is insufficient when dealing with single crystals because crack initiation, propagation, and crack path selection are phenomena that occur at the atomistic scale. A study of dynamic fracture in silicon, therefore, requires studying silicon at the atomistic scale.

Classical inter-atomic potentials, like the Tersoff potential, are not able to simulate silicon brittle fracture behavior that corresponds to experimental data [9, 10]. Mattoni 2007 [11] describes a method to use a modified Tersoff potential that is able to predict brittle fracture strength for group-IV materials. The method is not perfect, however, as it does not allow simulating thermodynamic ensembles at finite temperatures.

In Buehler 2006 [12], it was shown that a hybrid model consisting of ReaxFF and Tersoff potentials is able to reproduce experimental results accurately. When applied to covalently bonded materials like Silicon, the Tersoff potential, and other similar potentials, are unable to correctly model high-strain phenomena. The ReaxFF potential is able to provide QM accuracy [13], but at a computational expense approximately ten times larger than Tersoff. The development of the Computational Materials Design Facility (CMDf) [14] has been able to offset this disadvantage. At low strains, the Tersoff and ReaxFF potentials provide coincidental

descriptions of the atomic behavior and energy landscape in silicon (*Figure 1*). By combining the Tersoff and ReaxFF potentials, using each at the low-strain and high-strain regions respectively, an accurate and computationally efficient multi-scale simulation is possible. Buehler et al. 2008 [8] has shown that the CMDF hybrid model is effective at simulating dynamic fracture of silicon under both mode I and mode II loading conditions.

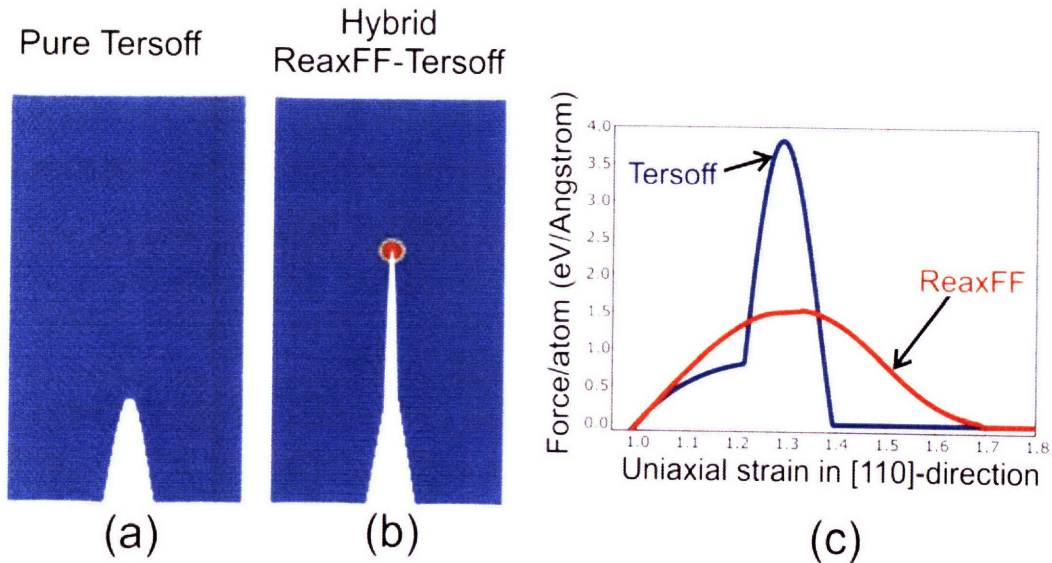


Figure 1: Crack propagation with a pure Tersoff potential (a) and the hybrid ReaxFF-Tersoff model (b) along the [110] direction. The blue regions are Tersoff atoms, the red regions are reactive atoms. Subplot (c) shows the difference in large-strain behavior between Tersoff and ReaxFF. Both descriptions coincide at small strain. Reprinted with permission from [12].

2.2 Modeling the Brittle-Ductile Transition

The brittle-ductile transition in silicon has been studied both through experiments, computer simulations, and numerical models. Thus far, there have not yet been any observations of BDT in a fully atomistic simulation. In 1993, Michot and George [15] showed that the nucleation of dislocation loops at a crack tip is involved during the formation of a plastic zone ahead of the crack tip. The dislocation nucleation event is hypothesized to be linked to the BDT. The formation of a plastic zone ahead of a crack tip is a feature of continuum mechanics, which requires that a plastic zone arises ahead of a crack tip to relax the high stress concentration there. The paper [15] shows that continuum mechanics is not sufficient in describing the events that may lead to ductile failure in the event of dislocation nucleation.

For pre-cleaved silicon single crystals, the BDT temperature is proportional to the exponential of $1/T_C$,

$$\frac{d\delta}{dt} \propto e^{-Q/kT_C} \quad (1)$$

where T_C is the transition temperature. This relationship between the opening rate and the transition temperature was discovered by St. John in 1975 [16]. The transition temperature ranged from 973K to 1223K, with an activation energy close to 2 eV. This experimental study provides a proven starting point for the modeling of the BDT using modern computational methods.

Michot [17], in a later paper in 1999, shows that there is a link between a material's ability to generate and move dislocations, and the material's BDT. The BDT is not constant for all samples of single crystal silicon. The quality of the cleavage surface has a major impact on the emission of dislocations. Michot found that the nucleation sites for dislocations are primarily defects along the crack tip. As the quality of the cleavage surface improves, the BDT temperature is shifted positively. Michot, however, concedes that there is little known about the nature of dislocation nucleation and the mechanisms by which the emission of dislocations occurs near the crack tip.

These past studies have provided a good understanding of the BDT, yet the fundamental mechanics of the process had not been discovered. In Xin 1997 [18] an attempt is made to create a numerical model that can simulate and characterize the process of the BDT in silicon single crystals. Xin uses a dislocation mechanics model, which considers the interaction between the crack and dislocations under an applied stress. The model developed considers a sample of single crystal silicon under constant mode I loading. It was found that at the BDT there is a sudden increase in dislocations at the crack tip, the plastic zone size increases, and for higher loading rates the BDT temperature increases. The presence of slip systems also was found to have an effect on the transition rate: increased number of active slip systems will increase the dislocation shielding effect, thus increasing the rate of transition.

Further studies have been done on the influence of slip systems on the BDT. Ferney 1999 [19] confirms the earlier finding in [18] that interactions between multiple slip systems will have an

effect on the rate of transition. The study concludes that the density and rate of dislocations and dislocation nucleation is influenced by the presence of multiple slip systems.

These studies, both experimental and numerical, provide a good background to begin further work in the study of silicon fracture. They confirm several known features of the BDT, but there is still a lack of fundamental understanding. To be able to fill in this gap of knowledge, it is necessary to complement the earlier studies with an atomistic examination, whereas detailed knowledge can be ascertained confidently.

3. Computational Methods

The key atomistic model used here is the ReaxFF force field, developed for silicon crystals. The present study uses two computational approaches to study the materials properties of single crystal silicon: CMDF and GRASP. CMDF is a novel computational facility that combines classical inter-atomic potentials with reactive inter-atomic potentials, creating a multi-scale, multi-paradigm approach to study fracture behavior in silicon [8, 12, 14, 20]. GRASP is a molecular dynamics package for complex force fields that is capable of carrying out parallelized simulations of large ReaxFF models. The software for GRASP was designed at Sandia National Laboratories. In this study, the ReaxFF reactive force field is implemented through GRASP to study high temperature failure of silicon.

3.1 Computational Materials Data Facility (CMDF)

CMDF was designed to provide a framework for multi-scale modeling that would enable the simulation of complex materials. CMDF is capable of providing a bridge from QM descriptions up to the continuum level [14]. In this study, CMDF is employed to provide a framework to study single crystal silicon with QM accuracy at the atomistic scale. A complete description of CMDF, including a description of the software and numerical methods can be found in [12, 14].

CMDF allows for a multi-paradigm approach to atomistic modeling. This study combines both classical empirical force fields with more accurate reactive force fields, Tersoff and ReaxFF respectively. The software uses a transition region to combine the two potentials, as shown in Figure 2. It has been shown that CMDF, in combination with the Tersoff and ReaxFF multi-paradigm model, provides an accurate description of brittle fracture in silicon single crystals [8, 12, 20]. The ReaxFF force field uses parameters derived only from QM calculations and does not contain empirical parameters; ReaxFF has been tested successfully against QM results [13].

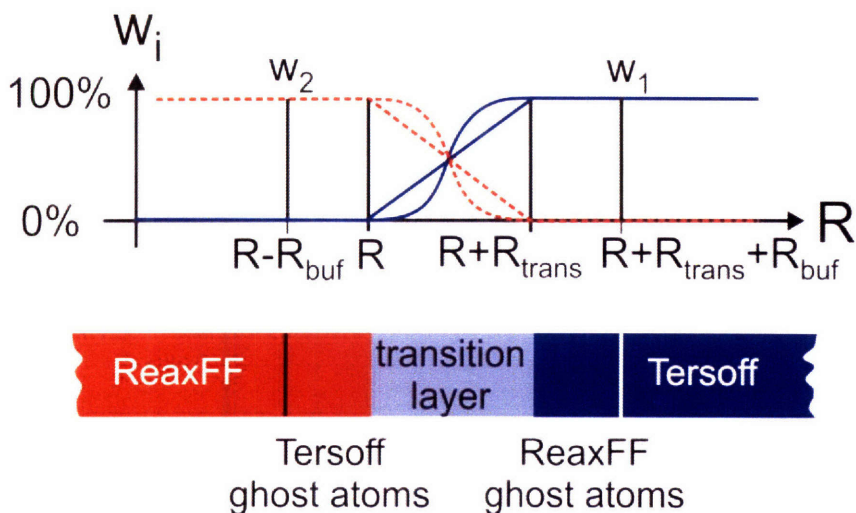


Figure 2: The CMDf software uses a transition region for simulations that employ multiple inter-atomic potentials for the description of atomic bonds and interactions. Shown here is the model used for combining the ReaxFF and Tersoff potentials in the simulation of a silicon crystal. Reprinted with permission from [12].

3.2 General Reactive Atomistic Simulation Program (GRASP)

CMDf provides a good framework for multi-paradigm modeling methods, but it is limited because it is executed serially. Increasing the size of the reactive region increases computation time—using only one CPU limits the size of the reactive region to about 1,000 atoms before computation time becomes several days to weeks in length. GRASP overcomes this disadvantage by allowing parallel execution of the code using the Message Passing Interface (MPI) standard. GRASP is used here to implement the ReaxFF force field for regions up to 20,000 atoms in size, by spreading out the computation over eight CPUs.

In order to study the brittle-ductile transition in silicon, it is necessary to create simulations that approach several hundred Kelvin of the melting point, 1687K [21]. It is hypothesized by the author of this thesis that a purely reactive approach to modeling the high-temperature failure incidences will allow for a more complete picture of any events that lead to the brittle-ductile transition. It is within this context that GRASP is used as a tool to model silicon behavior during high temperature mode I loading.

3.3 Method to Observe Mode I&II Brittle Fracture

To observe brittle fracture during mode I and mode II loading, a (111) system is created. The

crystal system is oriented such that there is a (111) fracture plane with initial [112] fracture direction. The x-y-z directions are $(1, 1, \bar{1}) \times (\frac{\bar{1}}{2}, \frac{\bar{1}}{2}, \bar{1}) \times (\frac{1}{2}, \frac{1}{2}, 0)$. A crack is initially created by inserting a V-shaped notch at the bottom edge of the crystal (*Figure 3*). Periodic boundary conditions are used in the z-direction to simulate non-free surfaces and create the plane-strain condition. The size of the system is $400\text{\AA} \times 560\text{\AA} \times 3.8\text{\AA}$, which is approximately 42,000 atoms. The size of the crack is $a=130\text{\AA}$.

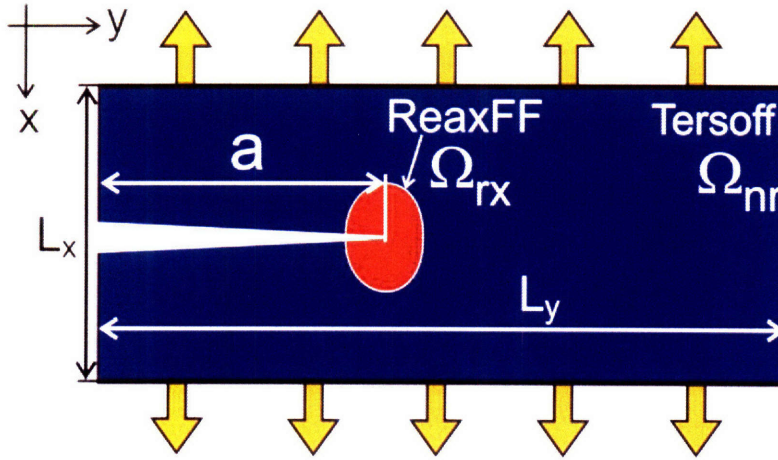


Figure 3: The crystal system is oriented such that there is a (111) fracture plane with initial [112] fracture direction. The x-y-z directions are $(1, 1, \bar{1}) \times (\frac{\bar{1}}{2}, \frac{\bar{1}}{2}, \bar{1}) \times (\frac{1}{2}, \frac{1}{2}, 0)$. The brittle fracture simulations use a crystal of size $L_x = 400\text{\AA}$ and $L_y = 560\text{\AA}$. The size of the V-notch crack is $a=130\text{\AA}$. Reprinted with permission from [12].

CMDf calculates the position and surface energy of every atom in the system each time-step, where the integration time step is $\Delta t=1\text{fs}$. The position of the crack-tip is updated every 20 integration steps based on an algorithm that finds atoms in a search region, then assigns the atom with the largest y-position as the crack tip. The atoms near the crack tip region are described with the ReaxFF force field; the entire reactive region is between 15-20 \AA in radius.

According to the type of strain system required, mode I or II, a load is applied by displacing the boundaries of the crystal. The crystals are all pre-strained with a tensile strain of 0.1% prior to beginning the simulation to account for thermal expansion of the crystal lattice. For this study, all the mode I and II brittle fracture tests were strained at a rate of 0.0001% or 0.00001% per femtosecond, held at a constant 300K. The temperature of the tests were held constant by the

use of a Berendsen thermostat [22].

3.4 Method to Observe Brittle-Ductile Transition

It is believed that the key to observe the BTD phenomenon it is required to simulate large systems over wide ranges of temperatures and strain rates.

Two separate methods of observation are implemented in the brittle-ductile transition tests. The first attempt to observe the brittle-ductile transition in silicon relies on the use of CMDF and the hybrid model based on Tersoff and ReaxFF force fields. The simulation technique is identical to that used for the simulation of mode I and mode II loading: the (111) crack system remains the same and the temperature as well as the strain rate is varied between tests.

The CMDF simulation may not reveal all the characteristics of the BDT because of the mixture of non-reactive and reactive force fields, and the relatively small reactive region (here small is used in terms of the length scales associated with dislocation nucleation, which typically requires much larger dimensions than brittle fracture, due to the formation of a plastic zone near the crack tip). GRASP simulations, therefore, are implemented to complement the CMDF simulations. The GRASP simulations describe atoms purely with reactive force fields, and therefore require significantly more computing power than the CMDF simulations. Parallel code execution and smaller crystal sizes were used to accommodate the increased computational requirement. GRASP calculates the position, velocity, energy, stresses, and forces on all the atoms within the simulation. The particle positions are output every 50 or 500 integration steps, where one integration step is $\Delta t=0.2$ fs.

The (111) fracture system used in the CMDF simulations is repeated for GRASP. (The crystal system is oriented such that there is a (111) fracture plane with initial [112] fracture direction. The x-y-z directions are $(1, 1, \bar{1}) \times (\frac{\bar{1}}{2}, \frac{\bar{1}}{2}, \bar{1}) \times (\frac{1}{2}, \frac{\bar{1}}{2}, 0)$.) The size of the system is $255\text{\AA} \times 525\text{\AA} \times 3.8\text{\AA}$, which is approximately 28,000 atoms. The initial crack length is $a=102\text{\AA}$. Periodic boundary conditions are used in the z-direction. The systems undergo mode I displacement at a constant strain rate of 0.0001% per fs.

It is possible that the periodic boundary conditions in the z-direction may limit the emission of

dislocations around the crack tip and surrounding defects, due to the constraints imposed on the dislocation mechanisms in the rather thin periodic slab. Simulations with a larger z-dimension are used for comparison, and to observe any changes that may occur due to changes in the sample thickness. These secondary simulations have a crystal size of $150\text{\AA} \times 296\text{\AA} \times 13\text{\AA}$ which maintains the number of atoms from the primary simulations of approximately 28,000 atoms. The initial crack length is $a=51\text{\AA}$.

Strain rate dependence is also explored by running simulations at much slower rates of displacement. Two simulations, at 300K and 1500K, are run at a shear rate of 0.00002% per fs, five times slower than the previous simulations. These simulations use the same parameters as the secondary simulations with larger z-dimensions.

4. Results

Continuum mechanics provides a suitable model to describe brittle fracture and failure at the macro-scale. Using CMDf and GRASP, a fundamental description of dynamic fracture can be created. The atomistic simulations presented here provide an ab initio approach to understanding the phenomena that lead to brittle fracture and the brittle-ductile transition. By observing the events that occur prior to crack extension,

The simulation results have all been visualized using the Visual Molecular Dynamics (VMD) software package [23, 24].

4.1 Crack initiation for mode I loading

Two simulations were setup to observe crack initiation during constant mode I loading. The two simulations ran at different strain rates, 0.0001% per fs and 0.00001% per fs. By running simulations at different strain rates, it is possible to observe if there is anomalous behavior caused by the strain rate.

Figure 4 shows the zoomed out view of the 0.0001% mode I test. It is possible to see the two simulation regions in this snapshot: the Tersoff non-reactive region in blue, and the ReaxFF reactive region in yellow. Focusing closer into the crack region, in yellow, relevant observations can be made.

Prior to crack extension, the crystal lattice begins to re-organize ahead of the crack tip. The formation of 5 and 7-member atom rings are observable (Figure 5), continuing earlier results seen in [20]. The equilibrium shape is hexagonal, with 6 member rings.

The second simulation, at a strain rate of 0.00001% per fs, demonstrates similar results, and allows for a reasonable assumption that the strain rate did not affect realistic crack growth phenomena.

During stable crack growth, the crack velocity (Figure 6) is consistent with earlier studies [20]. The stable crack growth velocity tends to approach approximately 3 km/s during mode I loading.

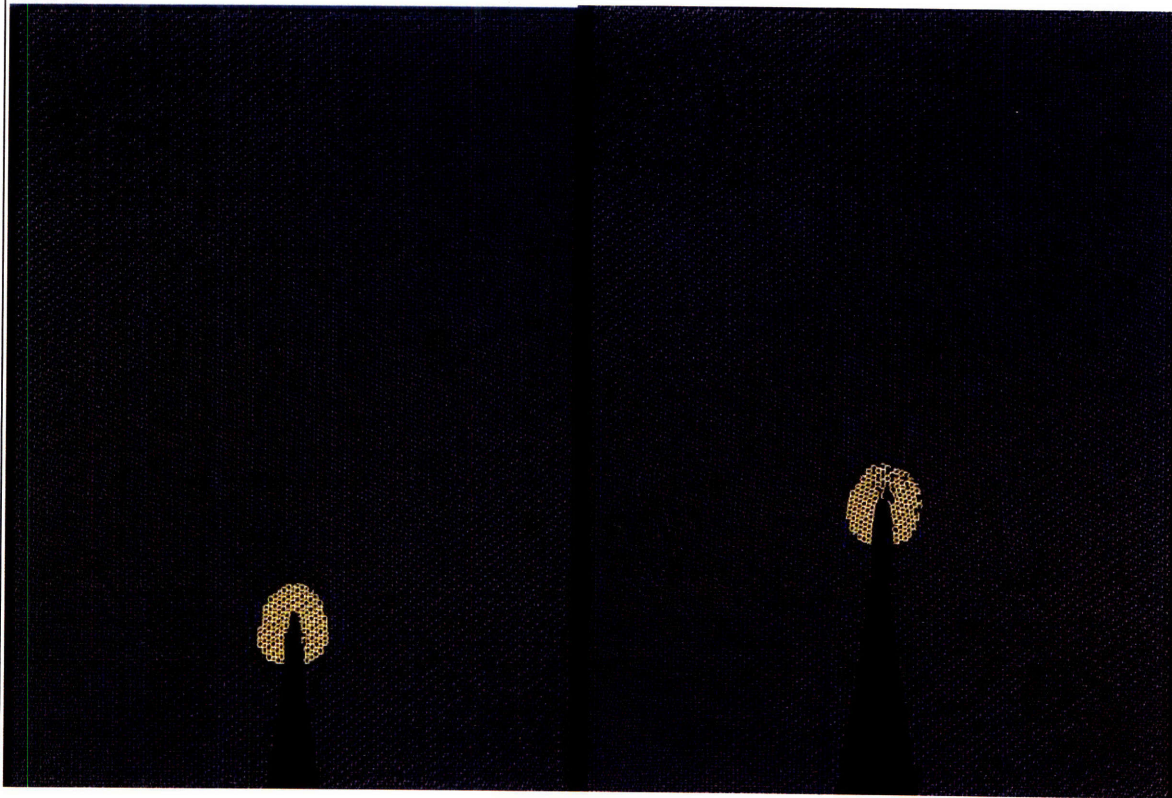


Figure 4: This snapshot is taken from a mode I loading simulation during crack extension. The reactive region can be seen in yellow, and the non-reactive region is shown in blue. The ReaxFF potential describes the atoms closest to the crack tip, and it is possible to zoom in closer and obtain more relevant data close to the crack tip. The snapshots are taken at 0.4581 ps (left) and 5.345 ps (right) . The strain rate for this simulation is 0.0001% per fs.

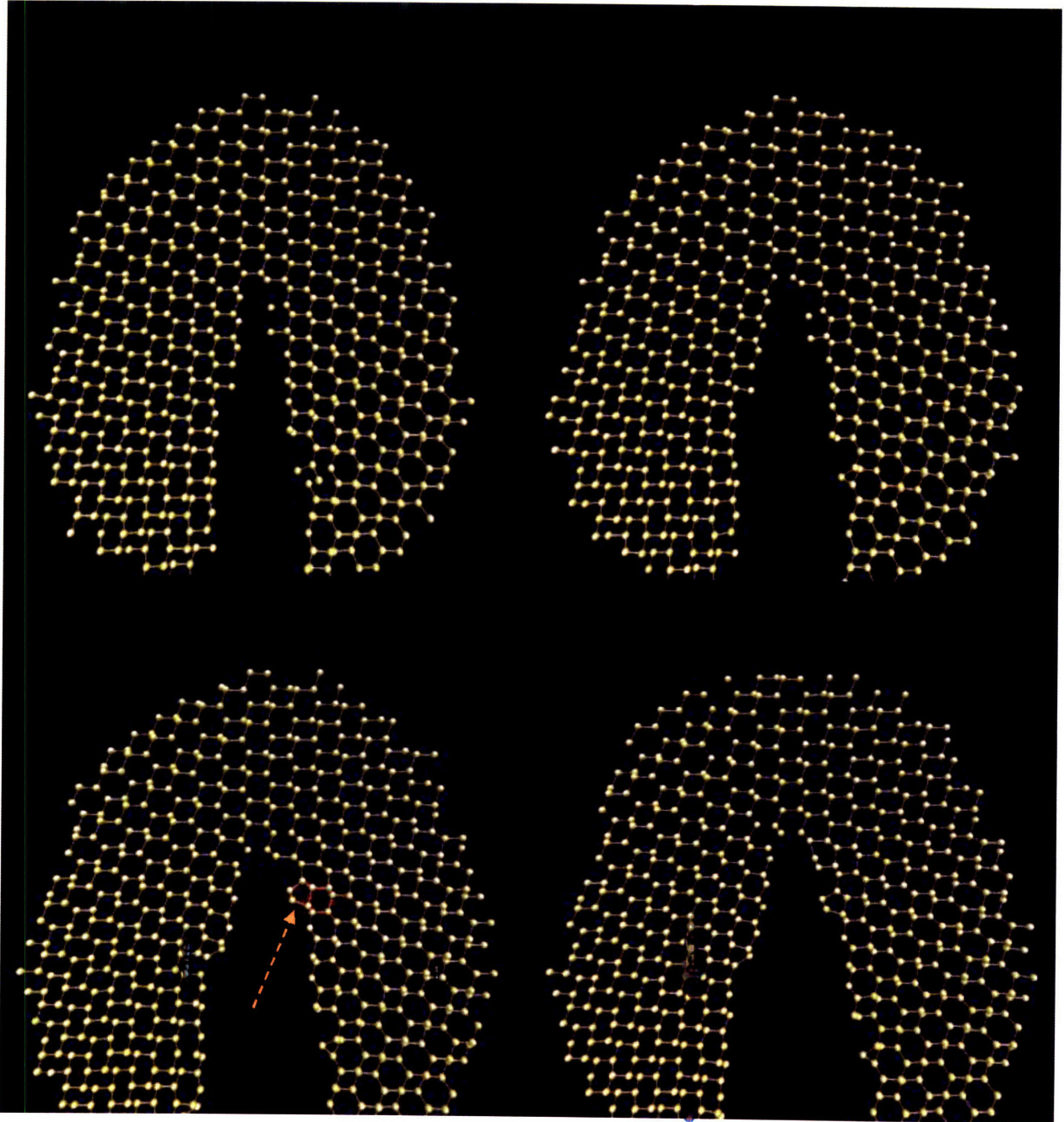


Figure 5: This snapshot is taken from a mode I loading simulation prior to crack extension. The reactive region is shown by itself: bond geometry and crystal structure can be obtained from this level of focus. At 1.0689 ps (bottom left) it is possible to see the formation of 5 and 7-member rings. One pair is highlighted in red. The snapshots are taken at .1527 ps (top left), 0.61098 ps (top right), 1.0689 ps (bottom left), and 1.6797 ps (bottom right). The strain rate for this simulation is 0.0001% per fs.

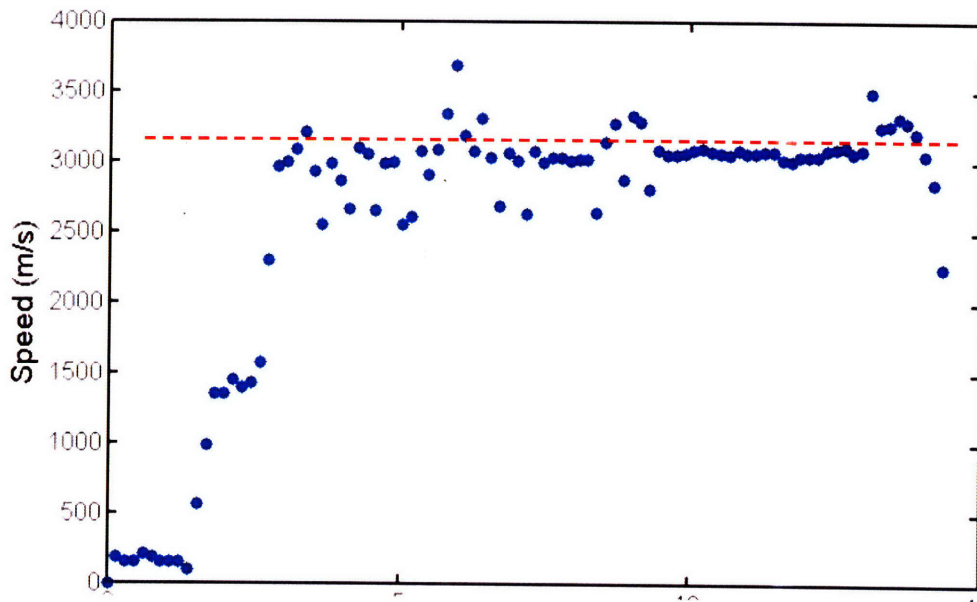


Figure 6: The steady-state crack velocity for the mode I loading case is approximately 3.3km/s (red dashed line). This result is taken from the time-averaged plot of the magnitude of the crack velocity. The observed crack speed is in the range of experimentally measured crack speeds for the same geometry [25].

4.2 Crack initiation for mode II loading

A similar procedure was used for mode II as for mode I: two simulations were run at different strain rates, 0.0001% and 0.00001% per fs. The results for the two tests had slightly different features. The slower (0.00001% / fs) simulation demonstrates behavior seen in the mode I tests: the formation of 5-membered rings (Figure 8). A significant feature of these simulations is that initial crack growth regime begins ahead of the crack tip, then suddenly changes direction, about 45 degrees to the left (Figure 7).

The faster (0.0001% / fs) simulation demonstrates 5 and 7-member ring formation as well. Another feature of this simulation is the formation of a void ahead of the crack tip prior to, and during, crack growth (Figure 9). This feature is not found in the slower (0.00001% / fs) simulation. During stable crack growth, the crack velocity (Figure 10) is consistent with earlier studies [8].

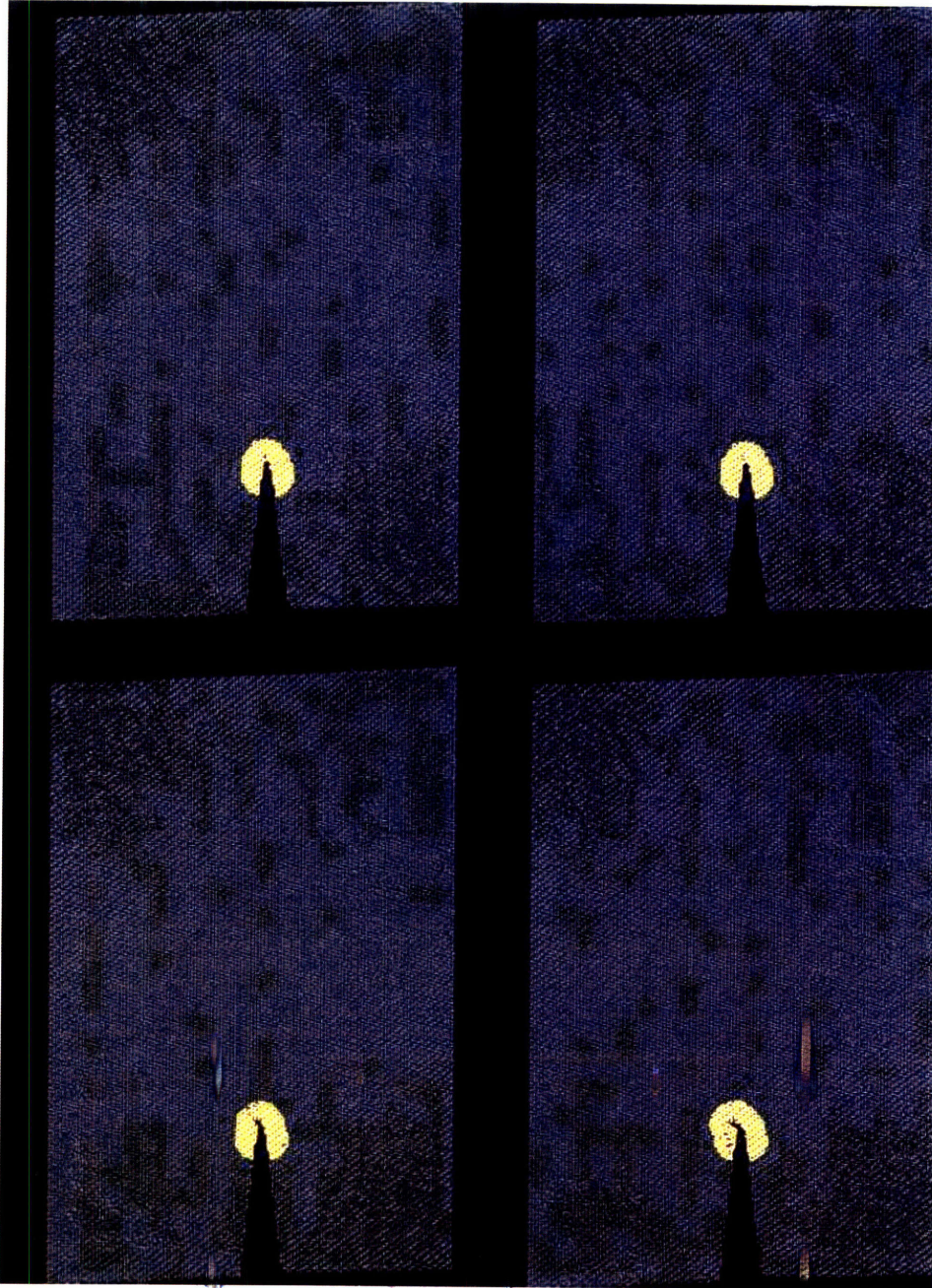


Figure 7: This snapshot is taken from a mode II loading simulation prior to crack extension. The reactive region can be seen in yellow, and the non-reactive region is shown in blue. The ReaxFF potential describes the atoms closest to the crack tip, and it is possible to zoom in closer and obtain more relevant data close to the crack tip. The initial deviation of the crack extension 45 degrees to the left can be observed in the bottom two snapshots. The snapshots are taken at 69.6312 ps (top left), 69.7839 ps (top right), 70.3947 ps (bottom left), and 70.8528 ps (bottom right). The strain rate for this simulation is 0.00001% per fs.

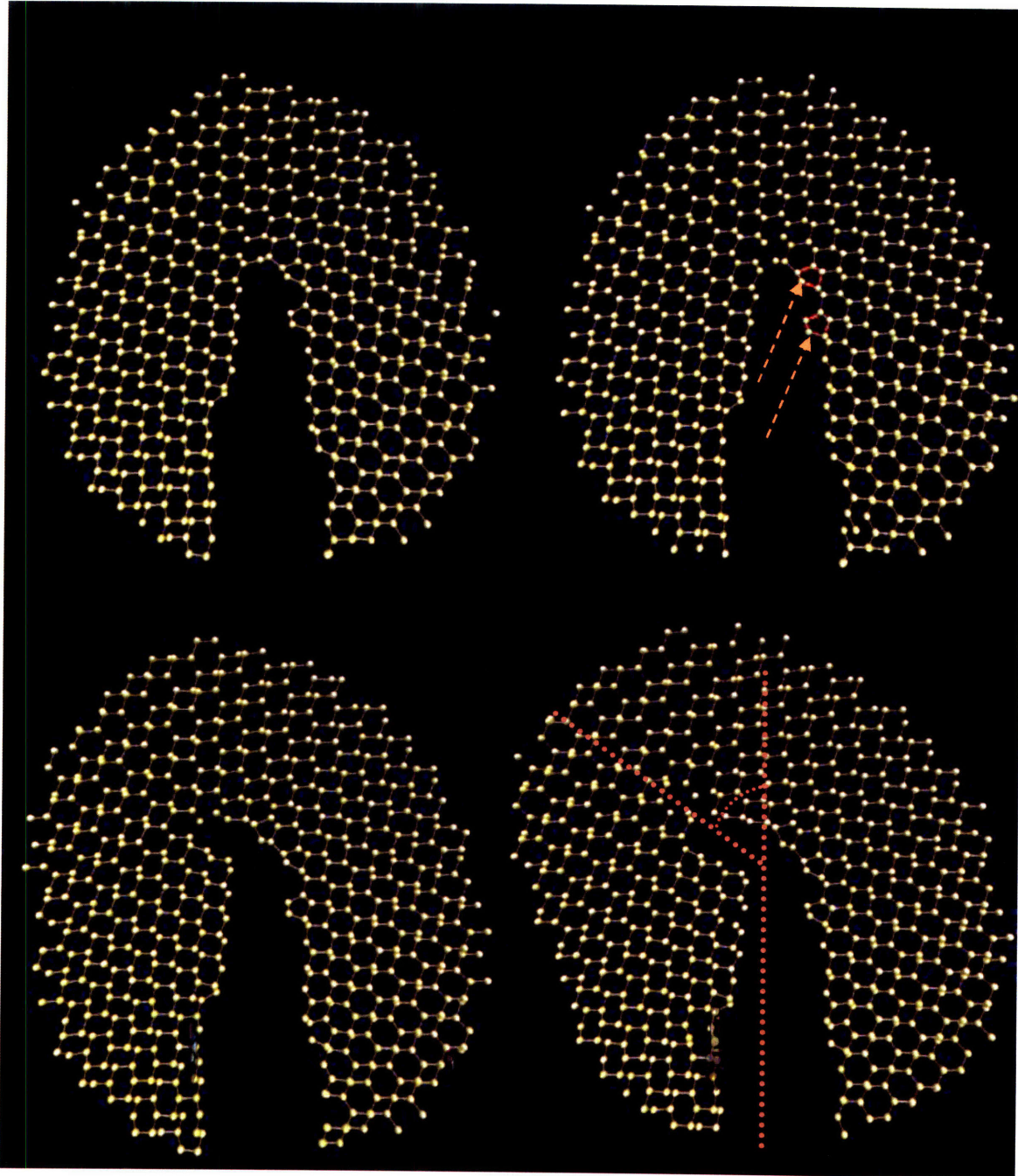


Figure 8: This snapshot is taken from a mode II loading simulation during crack extension. The angle of crack growth direction is approximately 30-40 degrees. The reactive region is shown by itself: bond geometry and crystal structure can be obtained from this level of focus. At 69.7839 ps (top right) it is possible to see the formation of 5-member rings. Two formations are highlighted in red. The snapshots are taken at 69.6312 ps (top left), 69.7839 ps (top right), 70.3947 ps (bottom left), and 70.8528 ps (bottom right). The shear strain rate for this simulation is 0.00001% per fs.

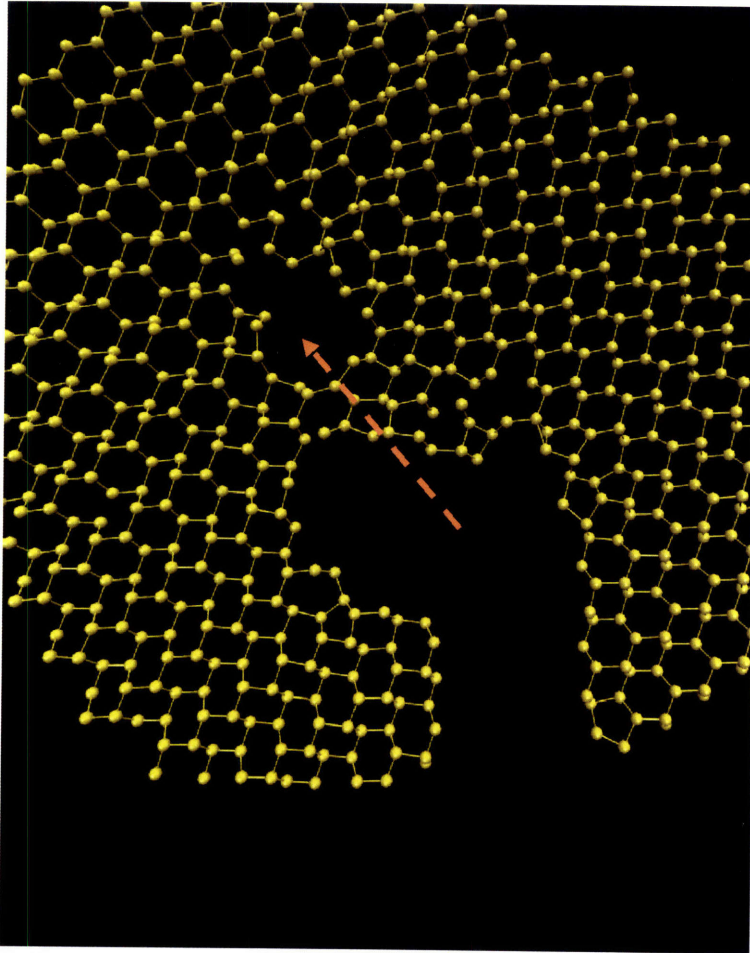


Figure 9: A void begins to form initially ahead of the crack tip before steady-state crack growth occurs. The arrow points towards the void, and is also pointing in the direction where crack extension will occur.

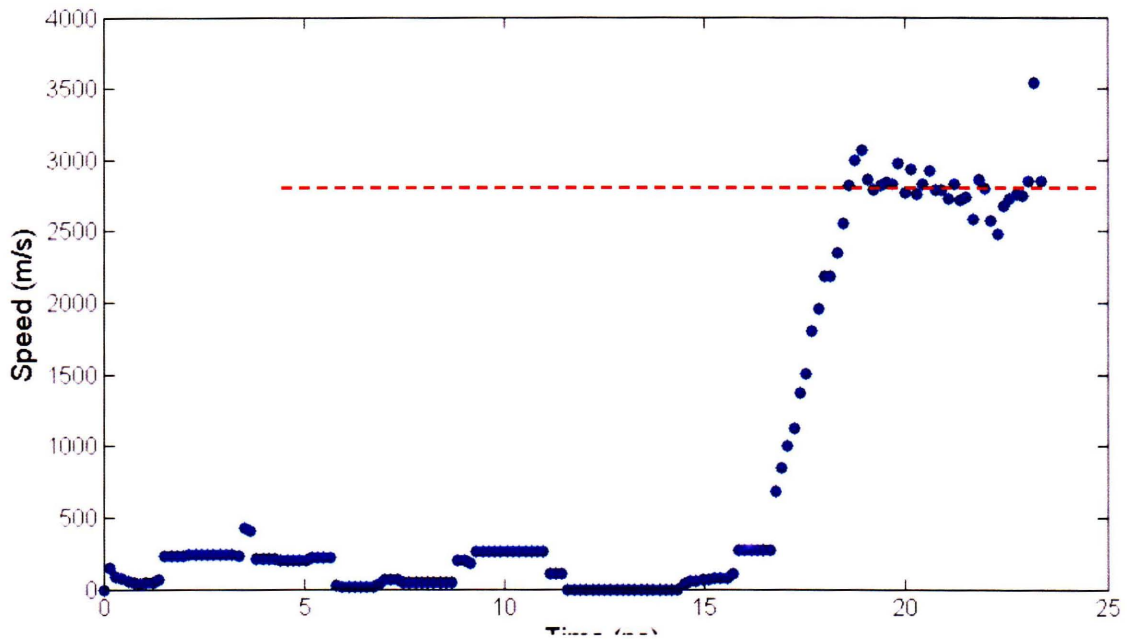


Figure 10: The steady-state crack velocity for the mode II loading case is approximately 2.8 km/s (red dashed line). This result is taken from the time-averaged plot of the magnitude of the crack velocity. The steady state velocity of mode II cracks is slightly slower than mode I cracks. Crack extension begins slightly after 15 ps, and steady-state crack growth occurs around 19 ps.

4.3a Brittle-to-Ductile Transition: CMDF Simulations

St. John [16] observed the brittle-ductile transition in silicon at temperatures between 900 and 1200K. Using these temperatures as a basis for simulation temperatures, CMDF simulations were carried out for temperatures of 700K, 900K, 1200K, and 1500K. A significant feature of these simulations is that they exhibit similar failure phenomena: void formation occurs above the crack tip, and void growth and coalescence drives crack extension (Figure 11). All the simulations are loaded at a strain rate of 0.00001% per fs.

There are not any significant differences between the simulations at the different testing temperatures. At higher temperatures, the crystal lattice appears to become more disordered, which could prohibit the use of CMDF simulations to model the BDT.

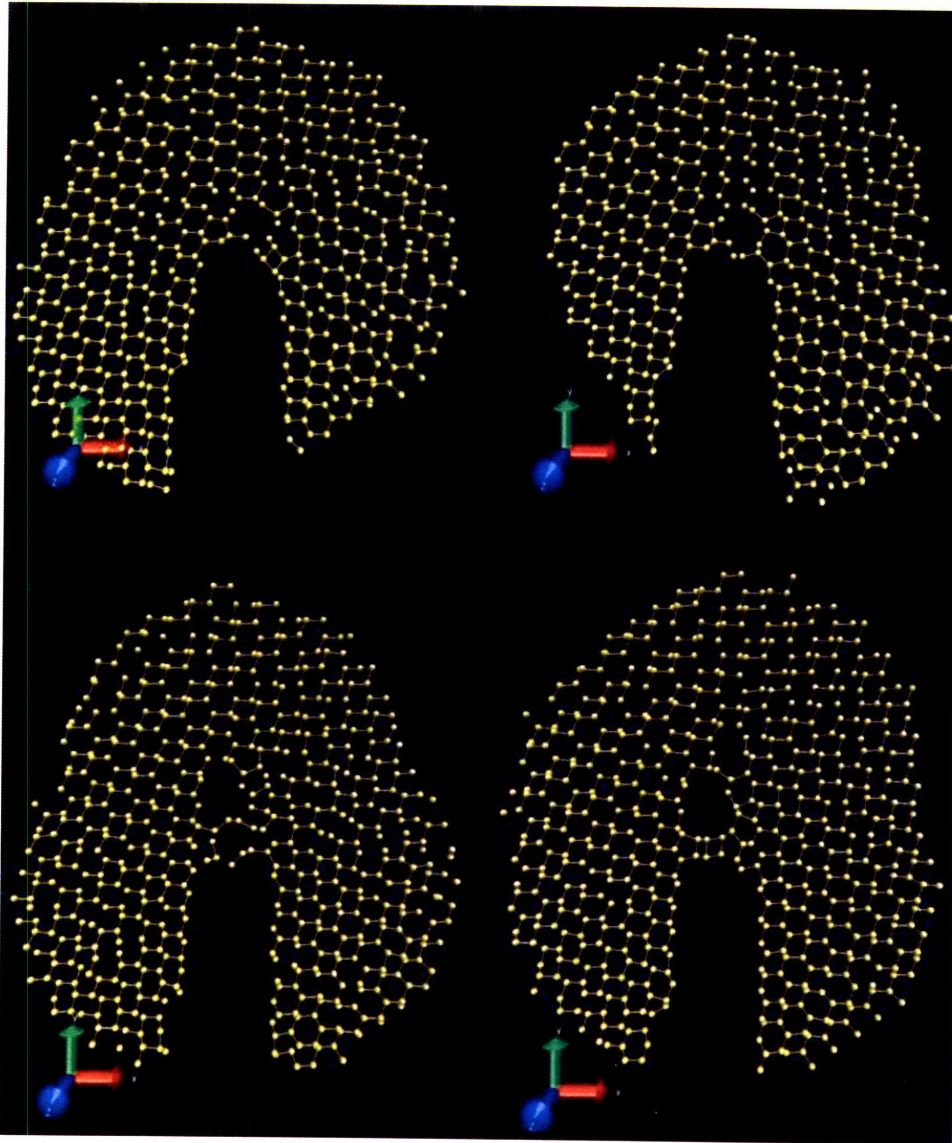


Figure 11: These snapshots are taken from a mode I test at 900K. The formation of voids occurs ahead of the crack tip prior to crack extension. At 18.7821 ps (bottom right) it is possible to see the formation of a secondary void ahead of the primary formation, the voids will coalesce and the crack will begin to grow. The snapshots are taken at 15.27 ps (top left), 16.0335 ps (top right), 17.5605 ps (bottom left), and 18.7821 ps (bottom right). The strain rate is 0.00001% per fs.

4.3b Brittle-to-Ductile Transition: GRASP Simulations

The results from GRASP differ slightly from the CMDf results. Due to limitations with VMD, with respect to the maximum number of atoms that can be visualized, it is not possible to draw the bonding structures; therefore, the visualizations shown in this section appear slightly different. The secondary simulations of the systems with the smaller x and y dimensions but

larger z dimension provide a better picture to analyze phenomena that can be observed visually.

The results for the 1200K simulation are indicative of brittle fracture (Figure 12). Key phenomena that should be observable during ductile failure, or the brittle-ductile transition, are the emission of dislocations from the crack tip, crack tip blunting, and failure due to shearing of the lattice, which are not observed in the 1200K simulation.

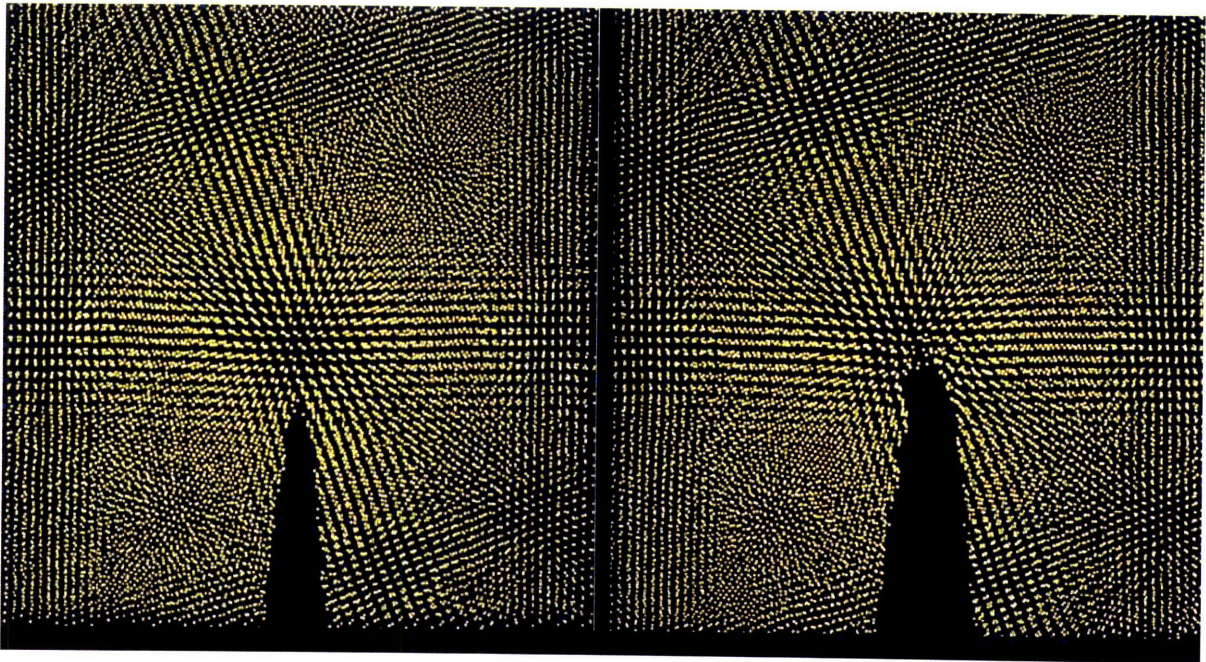


Figure 12: The events during the simulation of a silicon crystal under tension at 1200K are indicative of brittle fracture. There is no indication of a brittle-ductile transition. An interesting observation is the deviation of the crack path from the typical mode I crack direction. These snapshots were taken at 0 ps and 4.400 ps. At 4.400 ps the fracture event is taking place. This simulation has a crystal size of $150\text{\AA} \times 296\text{\AA} \times 13\text{\AA}$, approximately 28,000 atoms. The initial crack length is $a=51\text{\AA}$. The strain rate is 0.0001% per fs. The snapshots shown here are not of the entire crystal lattice, but are focused in closer to the crack tip for clarity.

At 1000K, void formation and coalescence can be observed (Figure 13). Crack growth begins around 6 ps and continues until the fracture regime changes from void formation to what might be ductile failure. At 1500K, the results are not very different from the lower temperatures. The snapshots in Figure 14 are taken on a longer timescale, to show the extent of crack growth that is not shown in snapshots of 1000K and 1200K. An interesting phenomenon is the deviation of the crack path from being straight, to angling several degrees to the left of the vertical. This phenomenon is apparent only at 1200K and 1500K, and cannot be seen in the 1000K simulation,

although it is possible that it may still be in effect but not as strongly. The crack path deviation was shown to occur at a 300K simulation with similar parameters; therefore, it cannot be concluded to be a temperature related effect.

Strain rate dependence is explored in the last set of simulations, at 300K and 1500K. These simulations had a strain rate of 0.00002% per fs, five times slower than the simulations prior to these. In Figure 15, visible shearing of the crystal lattice begins to occur at a plane inclined to the crack tip at about 30 degrees to the right with the emission of a dislocation. This is direct evidence for the atomistic mechanism of BDT, which is simulated here for the first time with MD. The strain rate is five times slower than the rate of the previous results. The failure mode of this sample is ductile, as cleavage does not occur in the simulation. Figure 17 shows a simulation at the same strain rate, but lower temperature (300K). Brittle fracture occurs as is expected based on other computational experiments.

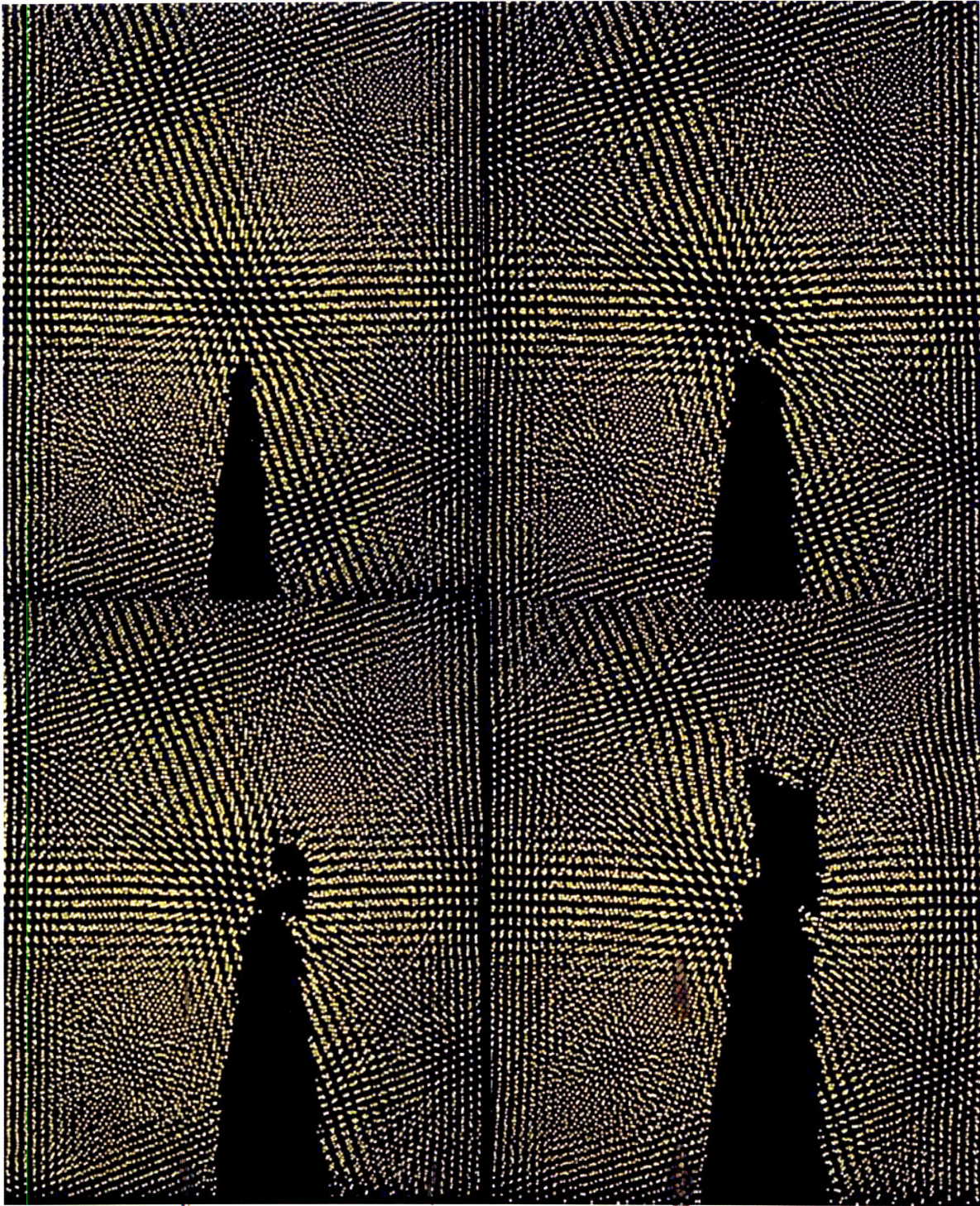


Figure 13: These snapshots are fracture events during a simulation at 1000K. The snapshots are carried out farther than was observed at 1200K. Void formation and coalescence can be seen at 5.570 ps (top right) and 6.700 ps (bottom left). At 8.700 ps (bottom right) it looks as if shearing of the lattice may be occurring, indicating a ductile failure mode. This simulation has a crystal size of $150\text{\AA} \times 296\text{\AA} \times 13\text{\AA}$, approximately 28,000 atoms. The initial crack length is $a=51\text{\AA}$. The strain rate is 0.0001% per fs. The snapshots shown here are not of the entire crystal lattice, but are focused in closer to the crack tip for clarity.

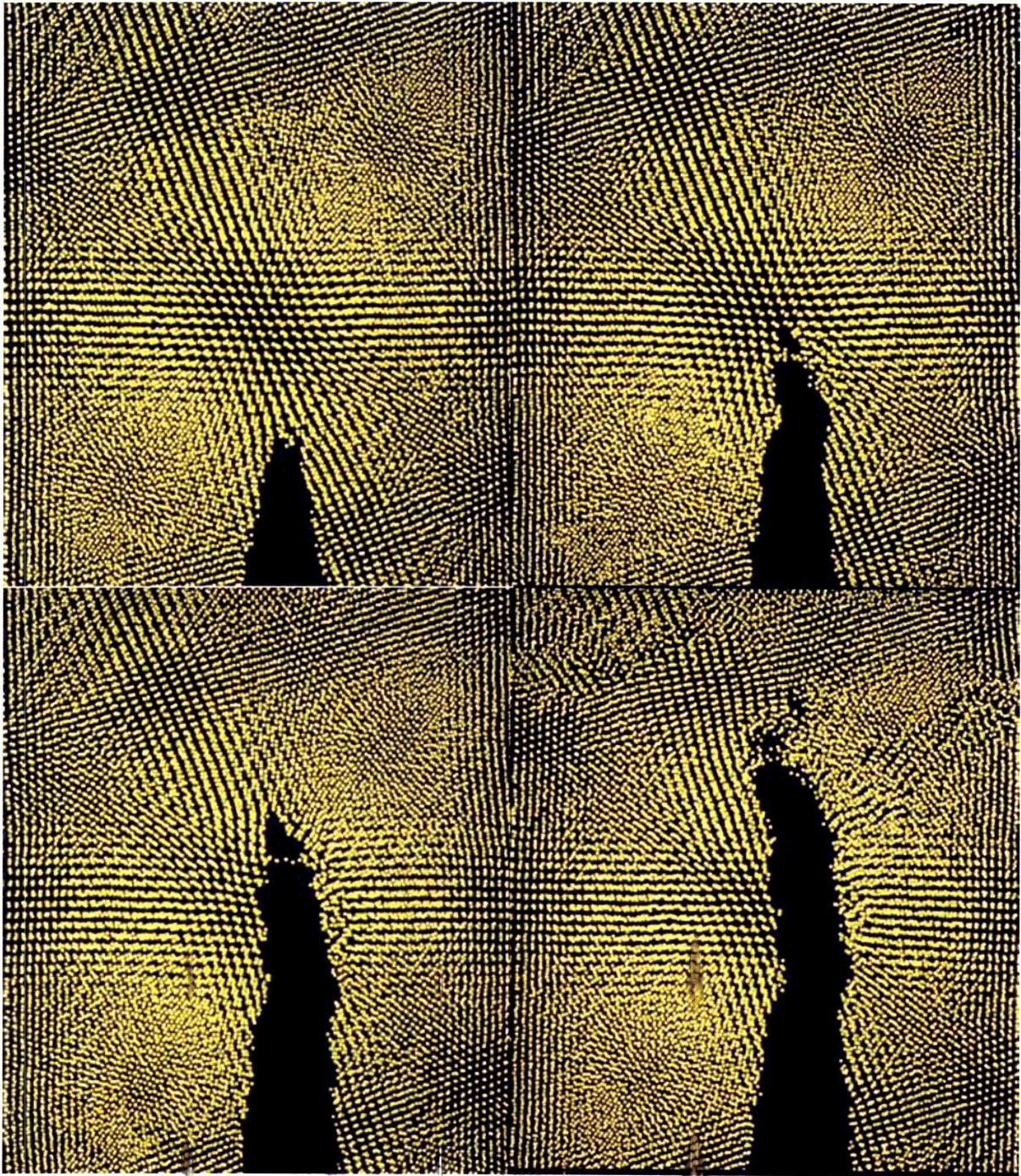


Figure 14: These snapshots are fracture events during a simulation at 1500K. At 5.290 ps (top left) crack tip blunting begins to occur. At 6.740 ps (top right) the process of void formation and coalescence begins to occur. Crack growth continues, but as in the 1200K and 1000K simulations, the crystal lattice begins to look more disordered and lattice shear may be occurring. This simulation has a crystal size of $150\text{\AA} \times 296\text{\AA} \times 13\text{\AA}$, approximately 28,000 atoms. The initial crack length is $a=51\text{\AA}$. The strain rate is 0.0001% per fs. The snapshots shown here are not of the entire crystal lattice, but are focused in closer to the crack tip for clarity.

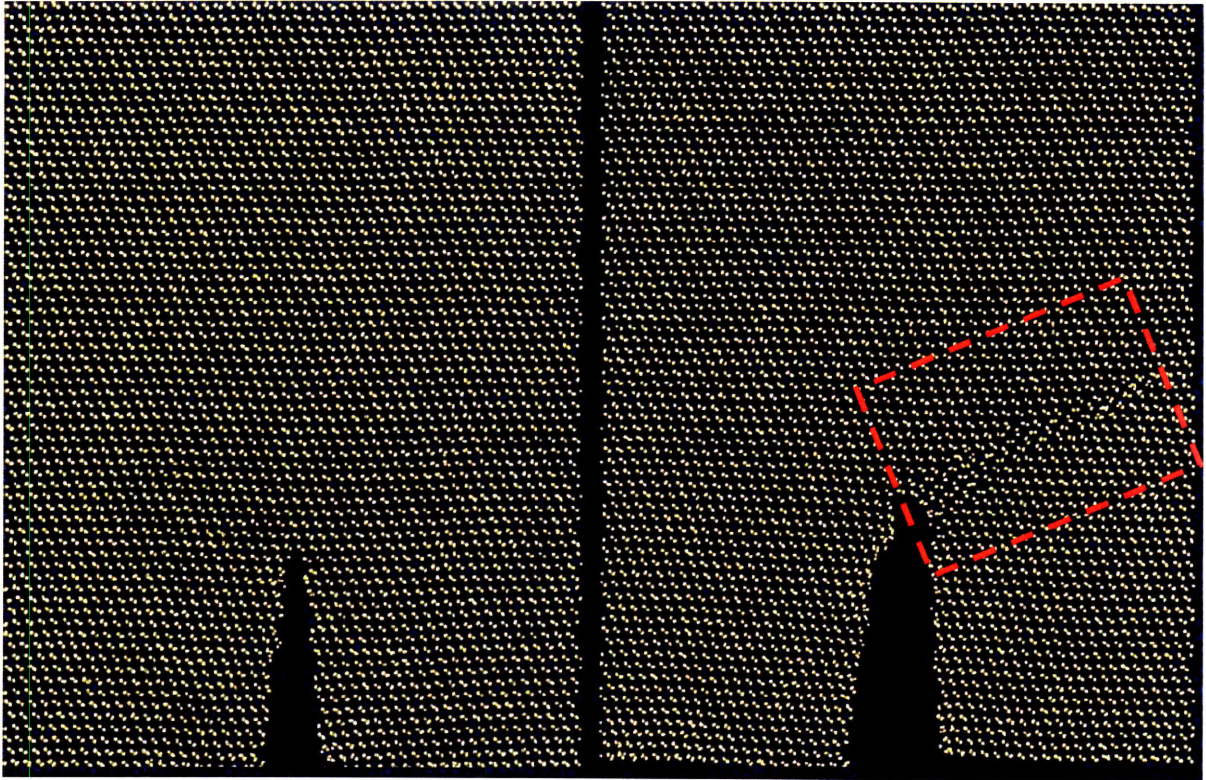


Figure 15: A simulation at 1500K, but slower strain rate, shows evidence of the BDT. The first snapshot is taken at 0 ps, prior to any displacement. After about 28 ps atomic movement begins to occur around the crack tip, and a dislocation is nucleated about 30 degrees to the right of the crack tip. The dislocation nucleation phenomenon is highlighted in the red square, clearly showing the local shearing of the lattice along the slip plane. The second snapshot is taken at 29.280 ps and the dislocation can be clearly seen. In this simulation, the strain rate is 0.00002% per fs, five times slower than the previous high temperature GRASP simulations.

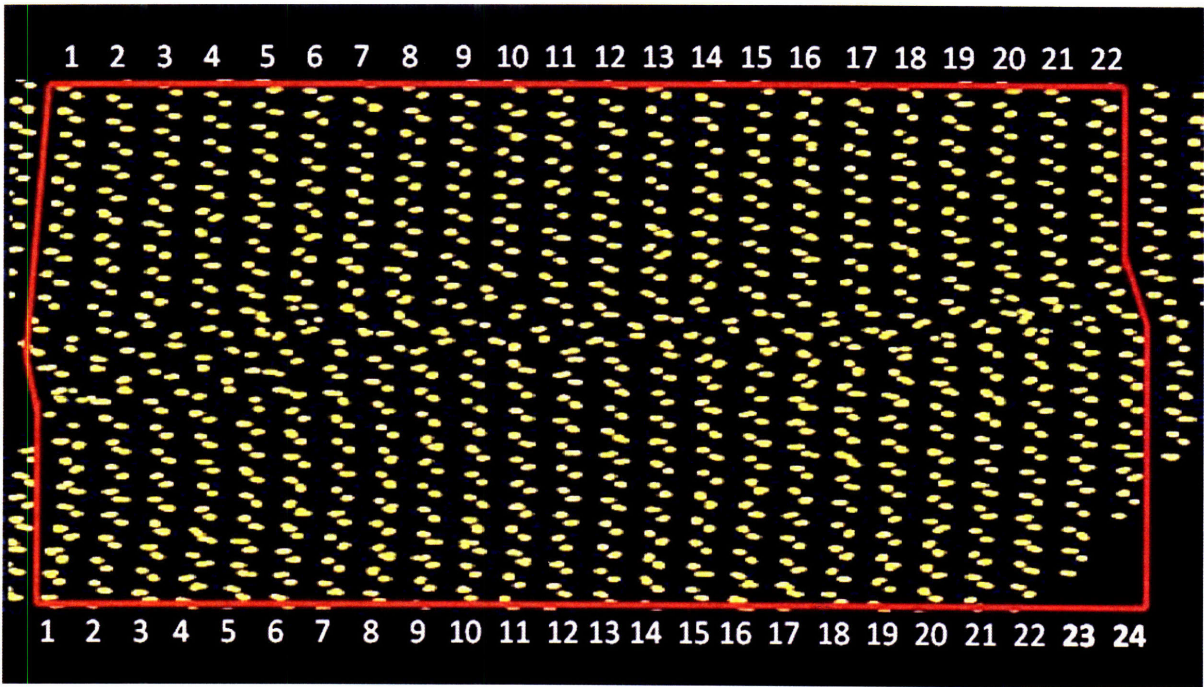


Figure 16: Shown here is the Burgers circuit drawn around the dislocation that is emitted at 29.280 ps. Additional half planes are inserted in the bottom part, clearly illustrating the nucleation of a dislocation. This is a distorted, focused snapshot of the highlighted area shown in Figure 15.

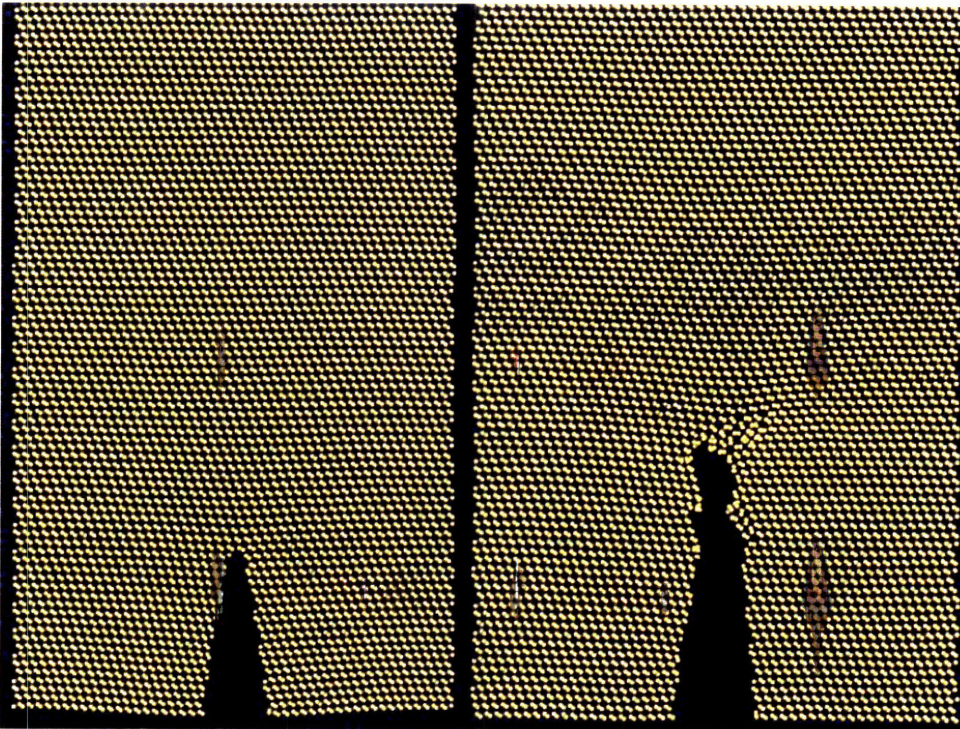


Figure 17: This snapshot of the 300K simulation at a mode I strain rate of 0.00002% per fs, shows that brittle fracture occurs via crack extension. This is the expected result, as the temperature is not high enough for a plastic zone to fully develop ahead of the crack tip and arrest crack propagation.

5. Discussion

5.1 Mode I & II Crack Growth During Brittle Fracture

In this section, the results of the mode I and mode II simulations are discussed in the context of earlier studies and continuum theory in general. The models used in the simulations conducted here have already been validated in previous studies of brittle fracture [8, 12, 14, 20], and therefore it is unnecessary to compare the current simulations with past experiments in brittle fracture. Instead, the analysis here will focus on the comparison of observed brittle fracture behavior and predicted behavior based on current theories for brittle fracture.

5.1.1 Asymptotic Stress Fields Analysis

Following is an analysis of the asymptotic stress field close to the crack tip, aimed at elucidating possible explanations for the differences in mode I and II loading. Continuum mechanics provides the relationships between displacement and stress, but not a description of material properties that determine these relationships. If it is possible, the combination of these atomistic studies and continuum theory could be viewed within the same context to form a complete picture, rather than competing pictures, of brittle fracture.

The branch of continuum theory that has been developed to describe the relationships between crack tip fields and the applied loads is known as Linear Elastic Fracture Mechanics (LEFM). LEFM theory provides a characteristic description of the stress fields ahead of the crack tip that is independent of material and lattice properties [5, 26]. The stress field ahead of the crack tip is asymptotic in nature, and a singular stress field exists at the crack tip. Given the coordinate system shown in Figure 18, the asymptotic stress field for a *stationary* crack during constant loading can be described as [5]:

$$\sigma_{ij} = \frac{K(t)}{\sqrt{2\pi r}} \Sigma_{ij}(\theta) + \sigma_{ij}^{(1)} + o(1) \quad (2)$$

Where $K(t)$ is the time-dependent stress intensity factor, r is the distance to the crack tip, $\sigma_{ij}^{(1)}$

is a contribution to the crack tip field of order unity, $o(1)$ is an asymptotic term¹, and $\Sigma_{ij}(\theta)$ is the angular variation of the stress field around the crack tip. The factor of interest in this asymptotic stress field analysis is the angular variations of the stress fields. The angular variation is given by the function $\Sigma_{ij}(\theta)$ and differs depending on the loading configuration (mode I or mode II). It is important to note that these asymptotic stress field calculations only describe the stress fields in the vicinity of the crack tip. The notion of a singular field at the crack tip edge is a non-physical assumption, but is rationalized through the concept of small-scale yielding [5]. The material surrounding the crack tip is assumed to be inelastic, and the supposedly singular stress field is assumed to be relieved through plastic flow. This point is very important in the later comparison of continuum theory with the observed simulation results.

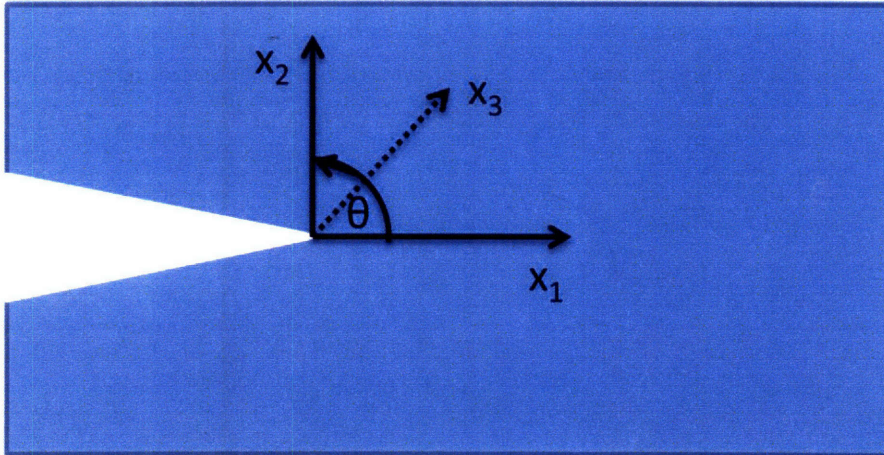


Figure 18: This is the coordinate system used for the LEFM asymptotic stress field model. The angle $\theta = 0$ is directly ahead of the crack tip on the x_1 axis.

The function $\Sigma_{ij}(\theta)$ for the mode I loading configuration is given by the equations [5],

$$\Sigma_{11}(\theta) = \cos \frac{1}{2}\theta \left\{ 1 - \sin \frac{1}{2}\theta \sin \frac{3}{2}\theta \right\} \quad (3)$$

$$\Sigma_{12}(\theta) = \cos \frac{1}{2}\theta \sin \frac{1}{2}\theta \cos \frac{3}{2}\theta \quad (4)$$

¹ $o(1)$ is a symbol used in the description of asymptotic series.

Weisstein, Eric W. "Landau Symbols." From MathWorld--A Wolfram Web Resource.

<http://mathworld.wolfram.com/LandauSymbols.html>

$$\Sigma_{22}(\theta) = \cos \frac{1}{2}\theta \left\{ 1 + \sin \frac{1}{2}\theta \sin \frac{3}{2}\theta \right\} \quad (5)$$

For mode II loading, the function $\Sigma_{ij}(\theta)$ is given by the equations,

$$\Sigma_{11}(\theta) = -\sin \frac{1}{2}\theta \left\{ 2 + \cos \frac{1}{2}\theta \cos \frac{3}{2}\theta \right\} \quad (6)$$

$$\Sigma_{12}(\theta) = \cos \frac{1}{2}\theta \left\{ 1 - \sin \frac{1}{2}\theta \sin \frac{3}{2}\theta \right\} \quad (7)$$

$$\Sigma_{22}(\theta) = \sin \frac{1}{2}\theta \cos \frac{1}{2}\theta \cos \frac{3}{2}\theta \quad (8)$$

The CMDF simulations do not provide a numerical description of the stress fields, therefore continuum theory and fracture mechanics can be tried to fill in the gaps. It is possible that the asymptotic stress fields may give some insight into the differences between mode I and mode II crack propagation. In Figures 19 and 20, the plots of the angular variations of the hoop, maximum shear, and maximum principal stresses for mode I and mode II stationary cracks are shown.

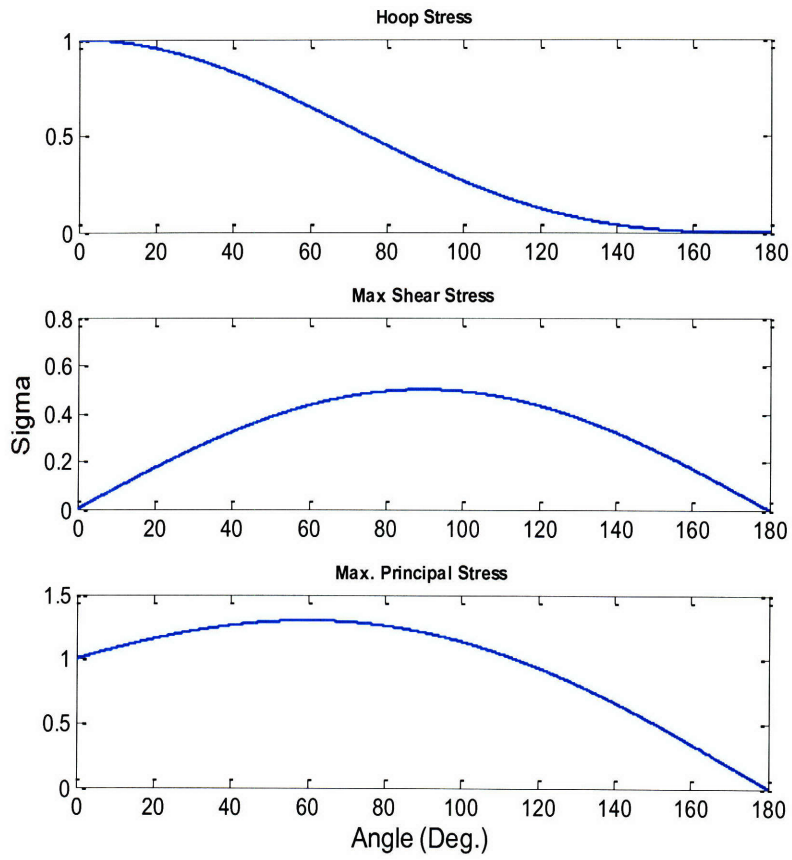


Figure 21: Angular variations (sigma) of the asymptotic stress field solutions for a stationary crack during mode I loading.

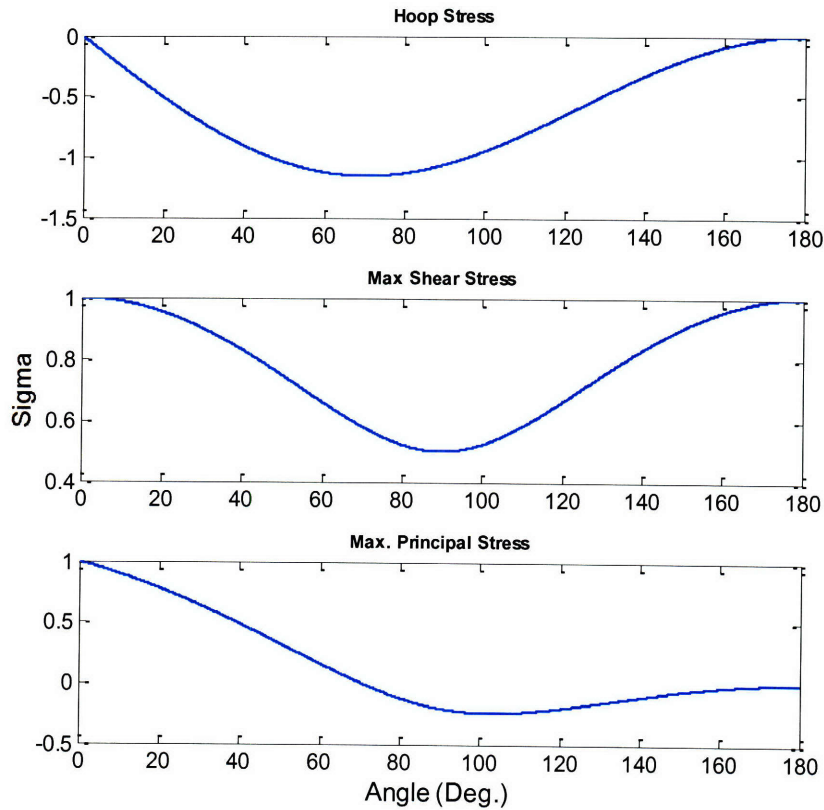


Figure 22: Angular variations (sigma) of the asymptotic stress field solutions for a static crack during mode II loading.

While the asymptotic stress fields provide a visual map for where loads tend to accumulate around the crack tip, they are not solely sufficient to describe the onset and direction of cleavage during brittle fracture. In single crystal silicon, cleavage tends to occur on one of a set of favored crystallographic planes, generally planes with high in-plane atomic density and maximum interplanar separation [7]. Crack initiation begins on the plane that first satisfies the Irwin energy criterion [5], specifically where the strain energy release rate is equal to the fracture energy for the system. The cleavage planes in silicon tend to be the $\{111\}$ and $\{110\}$ family of planes, whereas the (111) planes have lower fracture energy [27].

The question that arises when placing the results of the simulations in the context of fracture theory is, does the theory agree with the atomistic observations? In the simulations, structural reorganization of the lattice begins to occur prior to cleavage during both mode I and II loading, as shown in Figures Figure 5 and Figure 8. The mechanism for ring formation is unclear given the

current observations.

5.2 Brittle-Ductile Transition During Mode I Loading

Silicon is an intrinsically brittle material [28] with barriers that limit the transition from brittle to ductile failure modes. Intrinsically brittle materials have a barrier to the athermal emission of dislocations, preventing a fully-developed plastic zone from developing ahead of the crack tip, and the transition from brittle to ductile failure [29]. Experimental studies [15, 16, 29] and empirical micromechanical studies (as well as dislocation mechanics analyses) [18, 19] have shown that although the barrier to transition exists, silicon is able to transition from brittle to ductile behavior. Thus far, however, no direct atomistic simulation model that captures this effect has been reported, and to the best of our knowledge the results described in this thesis are the first of its kind. The BDT barrier involves silicon's inability to emit dislocations at the crack tip unless certain temperature and loading requirements are satisfied (specifically, silicon will only exhibit the BDT if temperatures are relatively high and the strain rate is relatively low) [29]. This barrier is effectively tested here: several simulations at a strain rate of 0.0001% per fs show signs of ductile behavior, but ultimately cleavage occurs, but at lower strain rates (i.e. 0.00002% per fs) the BDT occurs.

Fracture theory states that it is the formation of a plastic zone surrounding the crack tip that relieves the high stress concentrations that result from an applied load [26]. If a plastic zone does not develop, or does not develop fully, cleavage will occur. Plastic zone "shielding" arises from the nucleation, expansion, and multiplication of crack-tip dislocations. The sum result of the displacement fields of the individual displacements is a stress on the crack tip that counteracts the stresses resulting from an applied load [29]. Experimental and theoretical evidence says that dislocations will arise on specific slip planes, depending on the crystal structure of the material [9, 15, 17, 18, 29, 30].

While the phenomena of dislocation emission and expansion from the crack tip has been theorized and well documented in experiments as shown, there has yet to be a computational model that has successfully captured the event without a priori knowledge of the event itself. The results shown in Figure 15 and Figure 16 are direct evidence of the creation of an incipient plastic zone, in the form of a single dislocation being emitted from the crack tip. The dislocation

nucleates at an incline to the crack tip, suggesting the direction for the preferred slip plane is at around 30 degrees to the right of the crack tip. The key driver for dislocation nucleation is the accumulation of large resolved shear stresses on specific slip planes [6]. The continuum model in Figure shows that the peak of the maximum shear stress around the crack tip during mode I loading occurs at about 80 degrees (using the coordinates shown in Figure 18). This model closely coincides with the angle of inclination of the observed dislocation, which is slightly more than 60 degrees.

There is a clear distinction between the CMDF and GRASP results. Although the CMDF simulations are run at lower strain rates than the corresponding GRASP simulation where the BDT is observable, there are no signs of dislocation emissions. It is possible that the transition layer between the reactive and non-reactive regions is a barrier to dislocation emission, or that simply the size of the reactive region is too small in the CMDF simulations.

6. Conclusions

The most important contribution of this thesis is the direct simulation of the BTD mechanisms in silicon. Our results confirm, based on a fundamental, atomistic level of modeling that this phenomenon exists. The mechanism of this transition is a change from crack extension, the signature of brittle failure, to shearing of the lattice and the formation of dislocations, the signature of ductile failure. Future studies may be focused on quantifying the specific rate-temperature dependence of this phenomenon, thereby providing input parameters for continuum-type modeling.

Our studies have further shown a distinction of crack propagation in mode I versus mode II loading conditions. In mode I, the crack tends to grow straight, whereas in mode II, the crack branches off in a direction inclined to the initial crack. This phenomenon may be useful for the design of manufacturing techniques in which the loading mode may be used as a parameter to cut silicon into different crystal planes.

Overall, our results suggest that atomistic modeling with MD is a useful approach in studying key mechanical properties of silicon. Without using empirical parameter or input from experiment, such models provide a new paradigm in engineering science that may eventually be used for engineering design tools such as Computer Aided Engineering (CAE).

Bibliography

1. Haxel, G.B., J.B. Hedrick, and G.J. Orris. *Rare Earth Elements—Critical Resources for High Technology*. 2002 2005 [cited 2008 May]; Available from: <http://pubs.usgs.gov/fs/2002/fs087-02>.
2. Epstein, E., *The Anomaly of Silicon in Plant Biology*. 1994. **91**(1): p. 11-17.
3. Nielsen, F.H., *Nutritional requirements for boron, silicon, vanadium, nickel, and arsenic: current knowledge and speculation*. *Faseb J*, 1991. **5**(12): p. 2661-7.
4. Craighead, H.G., *Nanoelectromechanical Systems*. 2000. **290**(5496): p. 1532-1535.
5. Freund, L.B., *Dynamic fracture mechanics*. Cambridge monographs on mechanics and applied mathematics. 1990, Cambridge ; New York: Cambridge University Press. xvii, 563 p.
6. Buehler, M.J., *Atomistic Modeling of Materials Failure*. 2008: Springer.
7. Sherman, D., *Aspects of rapid crack propagation in silicon*. *Fatigue & Fracture of Engineering Materials and Structures*, 2007. **30**(1): p. 32-40.
8. Buehler, M.J., A. Cohen, and D. Sen, *Multi-paradigm modeling of fracture of a silicon single crystal under mode II shear loading*. *Journal of Algorithms & Computational Technology*, 2007. **2**(2): p. 203-221.
9. Hauch, J.A., et al., *Dynamic fracture in single crystal silicon*. *Physical Review Letters*, 1999. **82**(19): p. 3823-3826.
10. Holland, D. and M. Marder, *Cracks and atoms*. *Advanced Materials*, 1999. **11**(10): p. 793-+.
11. Mattoni, A., M. Ippolito, and L. Colombo, *Atomistic modeling of brittleness in covalent materials*. *Physical Review B*, 2007. **76**(22): p. -.
12. Buehler, M.J., A.C.T.v. Duin, and W.A.G. III, *Multiparadigm Modeling of Dynamical Crack Propagation in Silicon Using a Reactive Force Field*. *Physical Review Letters*, 2006. **96**(9): p. 095505.
13. van Duin, A.C.T., et al., *ReaxFF(SiO) reactive force field for silicon and silicon oxide systems*. *Journal of Physical Chemistry A*, 2003. **107**(19): p. 3803-3811.
14. Buehler, M.J., et al., *The Computational Materials Design Facility (CMDf): A powerful frame-work for multi-paradigm multi-scale simulations*, in *Combinatorial Methods and Informatics in Materials Science*, M.J. Fasolka, et al., Editors. 2006. p. 327-332.
15. George, A. and G. Michot, *Dislocation Loops at Crack Tips - Nucleation and Growth - an Experimental-Study in Silicon*. *Materials Science and Engineering a-Structural Materials*

- Properties Microstructure and Processing, 1993. **164**(1-2): p. 118-134.
16. John, C.S., *The brittle-to-ductile transition in pre-cleaved silicon single crystals*. Philosophical Magazine, 1975. **32**(6): p. 1193 - 1212.
 17. Michot, G., M.A.L. de Oliveira, and G. Champier, *A model of dislocation multiplication at a crack tip: influence on the brittle to ductile transition*. Materials Science and Engineering a-Structural Materials Properties Microstructure and Processing, 1999. **272**(1): p. 83-89.
 18. Xin, Y.B. and K.J. Hsia, *Simulation of the brittle-ductile transition in silicon single crystals using dislocation mechanics*. Acta Materialia, 1997. **45**(4): p. 1747-1759.
 19. Ferney, B.D. and K.J. Hsia, *The influence of multiple slip systems on the brittle-ductile transition in silicon*. Materials Science and Engineering a-Structural Materials Properties Microstructure and Processing, 1999. **272**(2): p. 422-430.
 20. Buehler, M.J., et al., *Threshold Crack Speed Controls Dynamical Fracture of Silicon Single Crystals*. Physical Review Letters, 2007. **99**(16): p. 165502.
 21. *CRC Handbook of Chemistry and Physics (Internet Version 2008)*. 88 ed, ed. D.R. Lide. 2008, Boca Raton: CRC Press/Taylor and Francis.
 22. Berendsen, H.J.C., et al., *Molecular-Dynamics with Coupling to an External Bath*. Journal of Chemical Physics, 1984. **81**(8): p. 3684-3690.
 23. Humphrey, W., A. Dalke, and K. Schulten, *VMD: Visual molecular dynamics*. Journal of Molecular Graphics, 1996. **14**(1): p. 33-&.
 24. *VMD: Visual Molecular Dynamics*. 2008 April 23, 2008 [cited; Available from: <http://www.ks.uiuc.edu/Research/vmd/>].
 25. Hauch, J.A. and M.P. Marder, *Energy balance in dynamic fracture, investigated by a potential drop technique*. International Journal of Fracture, 1998. **90**(1-2): p. 133-151.
 26. Kanninen, M.F. and C.H. Popelar, *Advanced fracture mechanics*. Oxford engineering science series ; 15. 1985, New York: Oxford University Press. xv, 563 p.
 27. Perez, R. and P. Gumbsch, *Directional anisotropy in the cleavage fracture of silicon*. Physical Review Letters, 2000. **84**(23): p. 5347-5350.
 28. Rice, J.R. and R. Thomson, *Ductile Versus Brittle Behavior of Crystals*. Philosophical Magazine, 1974. **29**(1): p. 73-97.
 29. Gally, B.J., *Experimental investigation of the brittle to ductile transition in fracture of single crystal silicon*. 1999. p. 267 p.
 30. Hess, B., B.J. Thijsse, and E. Van der Giessen, *Molecular dynamics study of dislocation*

nucleation from a crack tip. Physical Review B, 2005. 71(5): p. -.